DISTRIBUTION STATEMENT A: Approved for public release; distribution is unlimited.

Sediment Flux and Trapping on the Skagit Tidal Flats and Instrumentation for Quantifying Nearshore Sediment Transport and Turbulence (DURIP)

W. Rockwell Geyer
Woods Hole Oceanographic Institution
MS 11, Woods Hole, MA 02543
phone: 508-289-2868 fax: 508-457-2194 email: rgeyer@whoi.edu

Peter Traykovski
MS 12, Woods Hole Oceanographic Institution
Woods Hole, MA 02543
phone: 508-289-2638 fax: 508-457-2194 ptraykovski@whoi.edu

David K. Ralston
MS 12, Woods Hole Oceanographic Institution
Woods Hole, MA 02543
phone: 508-289-2587 fax: 508-457-2194 dralston@whoi.edu

Award Number: N00014-08-1-0790 and N00014-08-10790

LONG-TERM GOALS

The long-term objective is to determine the hydrodynamic processes controlling sediment transport and the associated morphologic response on tidal flats.

OBJECTIVES

The objectives of our 2008-2009 research program were:

- quantify the influence of barotropic (tidal) convergence on the lower Skagit tidal flats as a mechanism of sediment trapping and creation of ephemeral mud and sand deposits;
- determine the role of density fronts in creating and transporting high-concentration sediment suspensions, and assess the influence of these processes on sediment deposition and short-term morphological change;
- distinguish the influence of wave-induced sediment transport from tidal/fluvial processes, and determine how variations in tidal, fluvial and wind/wave forcing alter the bedform geometry, transport pathways, surficial sediment characteristics and tide-flat morphology .

Report Documentation Page

Form Approved
OMB No. 0704-0188

Public reporting burden for the collection of information is estimated to average 1 hour per response, including the time for reviewing instructions, searching existing data sources, gathering and maintaining the data needed, and completing and reviewing the collection of information. Send comments regarding this burden estimate or any other aspect of this collection of information, including suggestions for reducing this burden, to Washington Headquarters Services, Directorate for Information Operations and Reports, 1215 Jefferson Davis Highway, Suite 1204, Arlington VA 22202-4302. Respondents should be aware that notwithstanding any other provision of law, no person shall be subject to a penalty for failing to comply with a collection of information if it does not display a currently valid OMB control number.

1. REPORT DATE **2009**	2. REPORT TYPE	3. DATES COVERED **00-00-2009 to 00-00-2009**

4. TITLE AND SUBTITLE **Sediment Flux and Trapping on the Skagit Tidal Flats and Instrumentation for Quantifying Nearshore Sediment Transport and Turbulence (DURIP)**	5a. CONTRACT NUMBER
	5b. GRANT NUMBER
	5c. PROGRAM ELEMENT NUMBER
6. AUTHOR(S)	5d. PROJECT NUMBER
	5e. TASK NUMBER
	5f. WORK UNIT NUMBER
7. PERFORMING ORGANIZATION NAME(S) AND ADDRESS(ES) **Woods Hole Oceanographic Institution,MS 11,Woods Hole,MA,02543**	8. PERFORMING ORGANIZATION REPORT NUMBER
9. SPONSORING/MONITORING AGENCY NAME(S) AND ADDRESS(ES)	10. SPONSOR/MONITOR’S ACRONYM(S)
	11. SPONSOR/MONITOR’S REPORT NUMBER(S)

12. DISTRIBUTION/AVAILABILITY STATEMENT
Approved for public release; distribution unlimited

13. SUPPLEMENTARY NOTES

14. ABSTRACT

15. SUBJECT TERMS

16. SECURITY CLASSIFICATION OF:			17. LIMITATION OF ABSTRACT	18. NUMBER OF PAGES	19a. NAME OF RESPONSIBLE PERSON
a. REPORT **unclassified**	b. ABSTRACT **unclassified**	c. THIS PAGE **unclassified**	**Same as Report (SAR)**	**11**	

APPROACH

This was the major field year of the Tidal Flats study. The remainder of this report describes the results of that field effort.

WORK COMPLETED

We deployed an array of instrument platforms on Skagit Flats during a 1-month observational interval in June, 2009. High-resolution surveys of the currents and suspended sediment distributions were conducted in concert with the deployments.

The deployment array (Fig. 1) was designed to distinguish the flow and sediment-transport processes in channels and on the flats as well as in different locations across the flats. The platforms (fig. 2, 3) at the lower channel and flats (stations 1-7) documented the tidal, fluvial and estuarine conditions on the flats. Station 8 provided the fluvial conditions at the Freshwater Slough distributary (the largest freshwater source to the southern flats). All of the stations had accompanying surface moorings with TS/OBS sensors, to quantify baroclinic salinity and sediment gradients.

The instrumentation at all quadpod stations measured acoustic profiles and optical point measurements of suspended sediment concentration, bed elevation, horizontal and vertical velocity, conductivity, temperature and depth. The acoustic profiles of sediment concentration and bed elevation were measured with Acoustic Backscatter Sensors (ABSs) and Pulse Coherent Doppler profilers. Each of the pods had 1 or 2 Acoustic Doppler Velocimeters (ADVs, with pressure sensor) sampling 20 (and in some cases 50) cm above the bed for measurements of tidal currents, waves and turbulence. Much of this equipment was purchased with DURIP funds and the pulse coherent Doppler profilers were developed with DURIP funding.

Shipboard surveys were also conducted with a shallow-draft vessel for 8 days during the 1-month deployment interval.

RESULTS

The data return was excellent—almost all of the sensors worked properly and provided high-quality data. There were minor problems with fouling due to benthic algae (*enteromorpha intestinalis)*, but most of the sensors remained clear throughout the deployment. During the strong spring tides at the end of the deployment period there was moderate scour at one of the quad-pods which caused it to shift its vertical datum by 10 cm, but otherwise the instruments were stable. During June 2009, the river discharge ranged from its year-to-date maximum of 930 $m^3 s^{-1}$ in early June to about 450 $m^3 s^{-1}$ by the end of the month. The observation period spanned two spring tides and a neap, with stronger spring tides occurring around the solstice. The maximum tidal range was 5 m and resulted in tidal currents reaching 1.2 m/s on June 24, while the minimum range was 2.5 m on June 15. Winds were generally light (mean wind speed 2.4 m/s; maximum 9 m/s on June 24). However there were periods of significant surface wave orbital motion, and there was a clear influence of tidal currents on the wave amplitude. Suspended sediment concentrations were generally low to moderate, except during peak spring tides, when significant resuspension of sand occurred. During the early high-flow period, there was a distinctive wash load in the surface layer. Quantification of suspended sediment concentrations via gravimetric analysis is presently underway.

An example of the magnitude and variability of the stratification is shown for station 1 on the lower flats (Fig. 3), but similar conditions were observed at the other stations. The period shown is the transition from neap to spring. During neap tides, stratification remained strong for most of each tidal cycle, with surface-to-bottom differences of ~25 psu. As tidal amplitudes and velocities increased, stratification decreased. Suspended sediment concentrations, as seen in acoustic and optical backscatter, also depended on tidal amplitude. Backscatter intensity remained weak through the neap tides, but increased substantially spring ebb tides (e.g., days 20-23). Early in each strong ebb, stratification remained strong and backscatter was low. The water column mixed as the stratified until midway through the subsequent strong floods. The backscatter dropped when the water column restratified mid-flood, and the near-surface velocity became strongly sheared.

The linked tidal variation in stratification, shear, and suspended sediment concentration was also apparent in the small-boat surveys of the tidal flats. Cross-flat surveys during spring tides found that after lower low tide the salinity gradient advancing across the flats during the flood was vertically well-mixed. Stratification began to develop on the upper flats around high water, and remained strong through the early part of the strong ebb. An example of the cross-flat distribution of salinity, velocity, and acoustic backscatter during a strong ebb is shown (Fig. 4). During transect 1 early in the ebb, the stratified region extended across most of the tidal flats. Velocities were highly sheared near the surface due to the stratification and river outflow, with currents of about 0.5 m s^{-1} in the surface layer and near zero in the lower layer. About 1 hour later, the stratification had broken down on the upper flats but remained on the lower flats; correspondingly, the backscatter signal was strong where the water column was well mixed. The transition point during this survey occurred near station 2, and the instruments there showed a similar transition from strong stratification and low sediment concentrations to well-mixed with high suspended sediment. By transect 3, the well-mixed, high-backscatter region extended to the edge of the flats.

Suspended sediment dynamics and stratified turbulence

The data collected on Skagit tidal flats offers a unique opportunity to examine the effects of salinity stratification on suspended sediment dynamics in a macrotidal environment. The multi-frequency pulse coherent Doppler measurements (Fig. 5) provide centimeter vertical resolution profiles of both mean flow and turbulence (via the 6 Hz sampling rate vertical velocity measurements from a downward aimed center transducer). These measurements are unique because the multi-frequency processing allows us to overcome the traditional range velocity ambiguities typically associated with pulse coherent Doppler profilers and still measure 1.3 m long profiles with mean velocities of ± 1 m/s (Fig. 6). The Acoustic Backscatter Profilers (Fig. 7) provide high quality backscatter measurements also with cm vertical resolution and the widely spaced frequencies (1.0 , 2.5 and 5.0 mHz) combined with Optical Backscattering Sensors at 4 locations in the water column will help differentiate scattering from turbulent microstructure, fine sediment and sand resuspension. Nortek Vector ADVs at two heights will allow point measurements of turbulent velocity spectra, and thus serve as a consistency check for the pulse coherent Doppler turbulence measurements. Salinity measurements are also available at 2 to 4 locations in the water column depending on the site location.

While all the pulse coherent Doppler (PC-Doppler) data have not been processed yet as we are iteratively optimizing the multi-frequency inversion initial examination of the overall data set and a few selected bursts shows very interesting results. In Figure 5, u (along channel), v (across channel) and w (vertical) velocity profiles are shown for data bursts during ebb tide (left panels), near slack low (center panels) and flood tide (right panels). There is a strong pulse (30 cm/s) of lateral flow off the

flats and into the channel during late ebb with a velocity reversal 20 cm above the bed (green solid line in profiles in upper-left panel). The ABS backscatter (Fig. 7, left lower panel) shows strong scattering from an interface located at 40 cm above the bed (cmab), which was confirmed to be a salinity gradient with salinity sensors (not shown). The difference in the height of the interface is due to the ABS burst was taken 20 min before the PC-Doppler data. Bursts taken at the same time show the same interface height. Interestingly, the fresh water above the interface has much higher backscatter levels due to either turbulence microstructure or fine suspended sediment. OBS data will be used to examine this further. The turbulence measurements (RMS vertical velocity profiles, Fig. 5 upper right panel) from the pulse coherent Dopplers during ebb show a near bed peak in turbulence, followed by suppressed turbulence at the interface 20 cmab and then increased turbulence in the upper layer. During slack tide the vertical velocity fluctuations are dominated by short period waves, with the expected rapid decay in vertical velocity. During flood tide the vertical velocity measurements show a much uniform structure, and the along channel flow has a logarithmic profile consistent with the absence of stratification as measured by the salinity sensors.

During the spring tide at the beginning of the deployment with strong river outflow the ABS measurements often show high backscatter in the upper water column associated with the fresh water (Fig. 7, left panels). Salinity stratification maintains a low-turbidity lower layer through the end of the ebb and into the flood tide when mixing results in more vertically uniform properties. During the spring tide towards the end of the deployment, more energetic conditions were present due to large tides and larger waves. During an ebb tide in this period (Fig. 5, right panels), the opposite situation from the previously shown ebb occurs, as stratification caps puffs of sand resuspension from mixing above 10 cm into the water column. These snapshots of data provide an indication of the quality of data available and show that there are many interesting processes that will be examined in the proposed work.

These measurements will allows us to examine the details of the interaction of stratified turbulence and vertical profiles of sediment concentration as the stratification approaches the seafloor. Presumably this is when stratification will have greatest effect on sediment transport as it can cap a suspension that otherwise extend high into the water column, and reduce bottom stress limiting resuspension. Combining the large scale shipboard survey data with the small scale quadpod data will allow us to examine to the roles of local mixing vs. advection of the salt wedge off the flats during the middle of ebb tide when conditions at a given site transition from stratified to well mixed. These results will have applications to many other environments with stratified turbulence and sediment resuspension, such as estuaries or river outflows into open shelf environments.

IMPACT/APPLICATIONS

This project will contribute both to the understanding of and the ability to measure key physical variables in shallow coastal environments of interest to the Navy. Our particular ability to resolve the vertical structure of the flow and water properties has important implications for the application of remote sensing to these environments—the conditions at the surface may not be relevant to the conditions at depth, even in water depths of 1-2 m. The project also provides essential ground-truth for the development of morphodynamic models, which the Navy will use in the future to forecast changes in bottom morphology and sediment rheology. From the DURIP funding we are able to purchase new equipment allowing the measurement described to be conducted and allowing similar measurements in the future. In particular, the development of the multi-frequency pulse coherent Doppler will allow

high resolution profiling even in extremely energetic conditions (flows > 1 m/s), which was not possible with previous technologies.

RELATED PROJECTS

Ralston is PI on a closely related project entitled “Sediment transport at density fronts in shallow water”, which involves modeling of the Skagit Flats using FVCOM. These two projects are tightly coupled. We are also collaborating closely with the other investigators in the DRI.

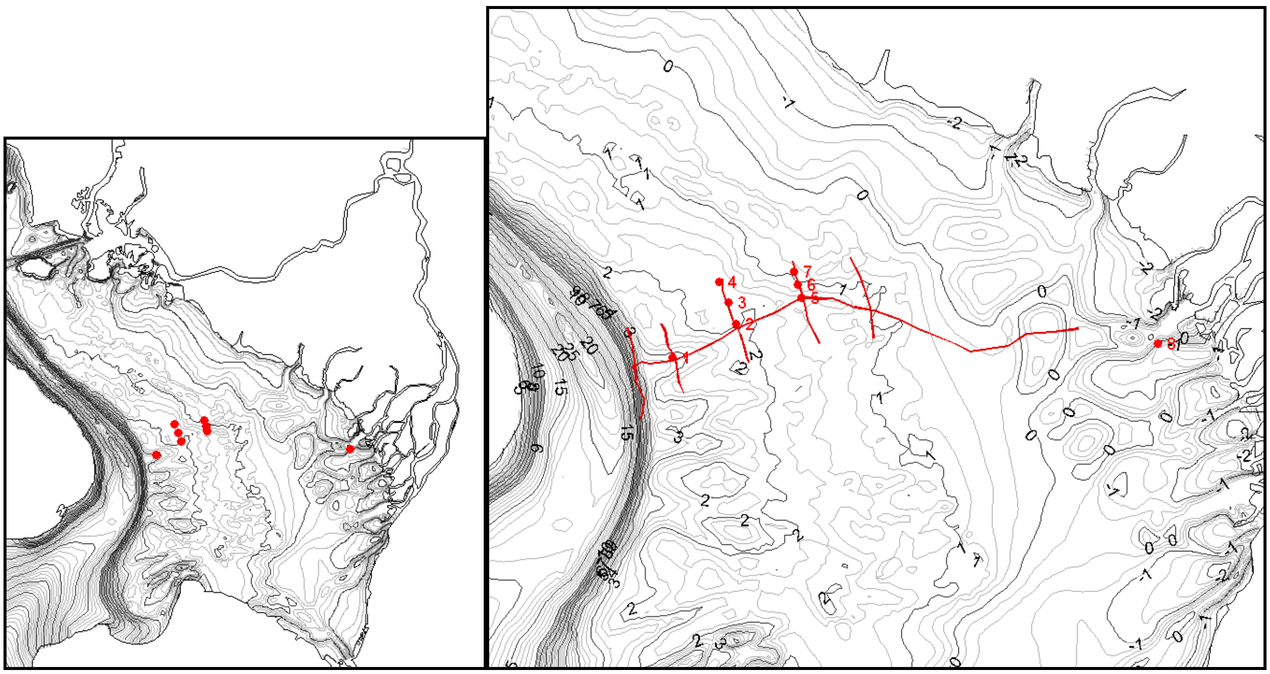

Figure 1. Bathymetry of the Skagit Bay tidal flats (left) with a zoom on the study area on the southern flats (right). Red dots indicate frame locations, and lines show across-flats and across-channel survey lines.

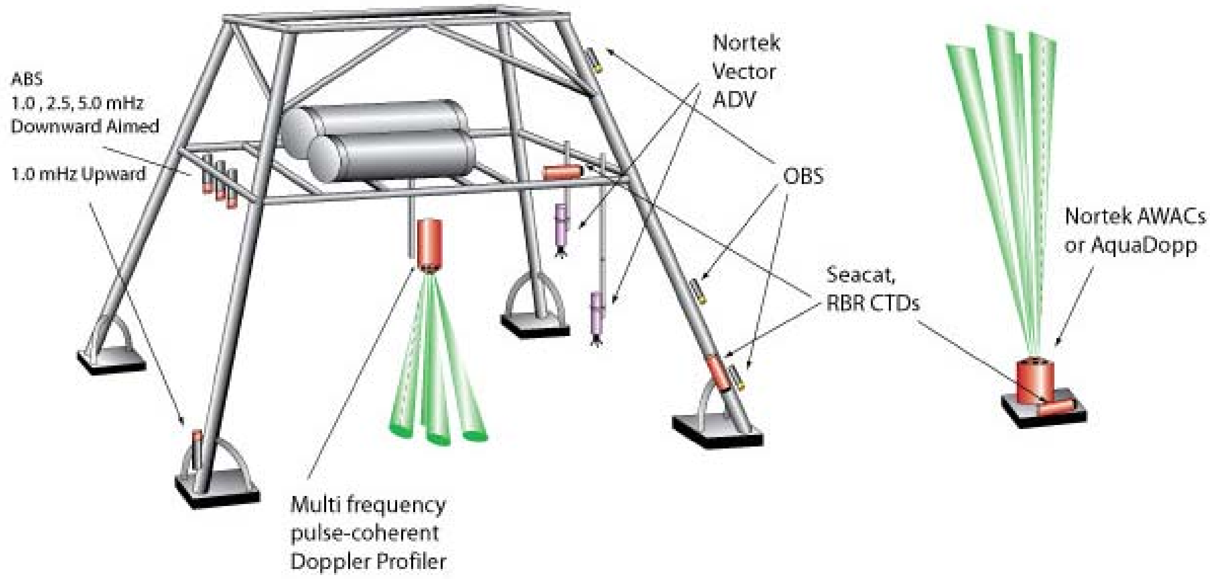

Figure 2. Schematic of quadpods showing a typical equipment configuration. Each quadpod was accompanied by a upward looking acoustics Doppler current profiler (ADCP) and a bottom mounted conductivity/temperature/pressure sensor.

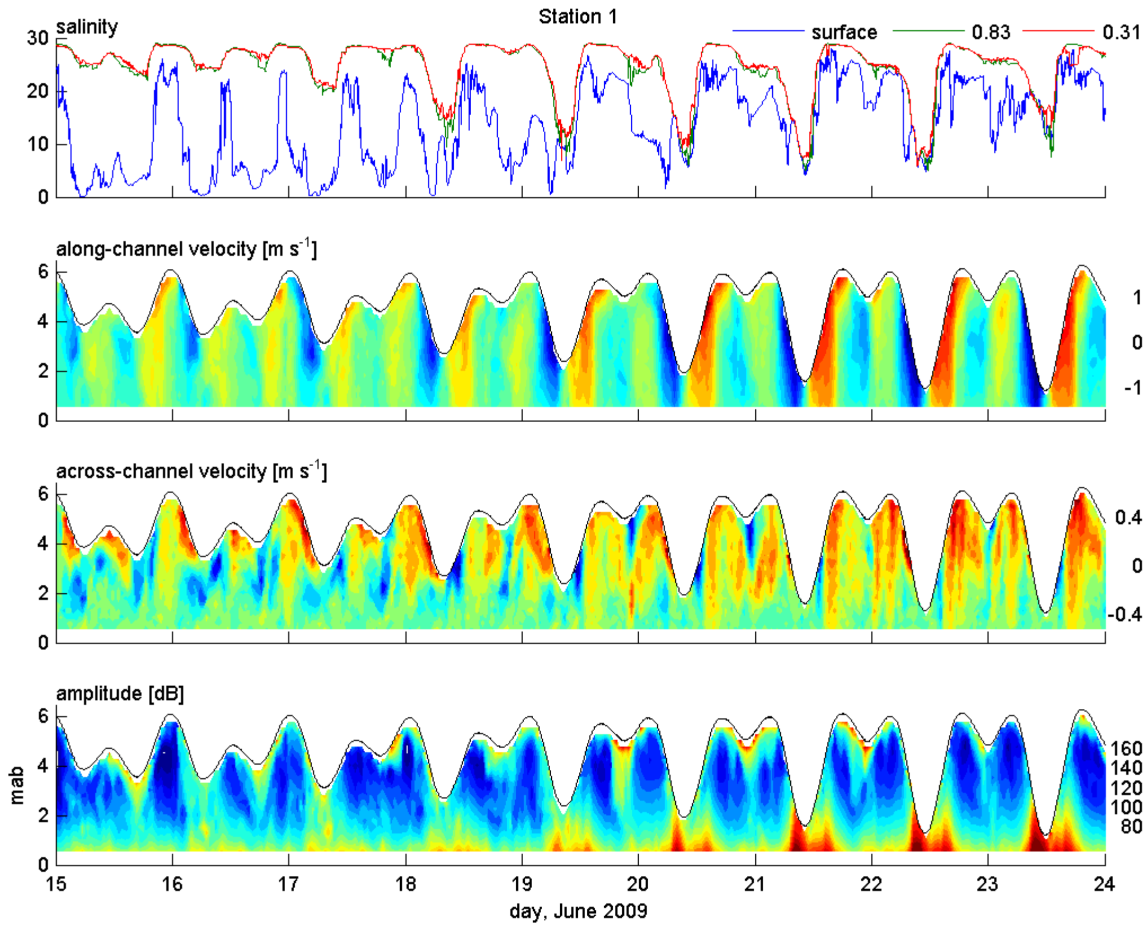

Figure 3. Time series of salinity (near-surface, 0.83 and 0.31 m above bottom), along-channel velocity, across-channel velocity, and acoustic backscatter at station 1 (location shown in Fig. 1) during the transition from neap to spring tides. Backscatter intensity is shown as a proxy for suspended sediment; optical backscatter sensors show similar spring-neap and tidal variability.

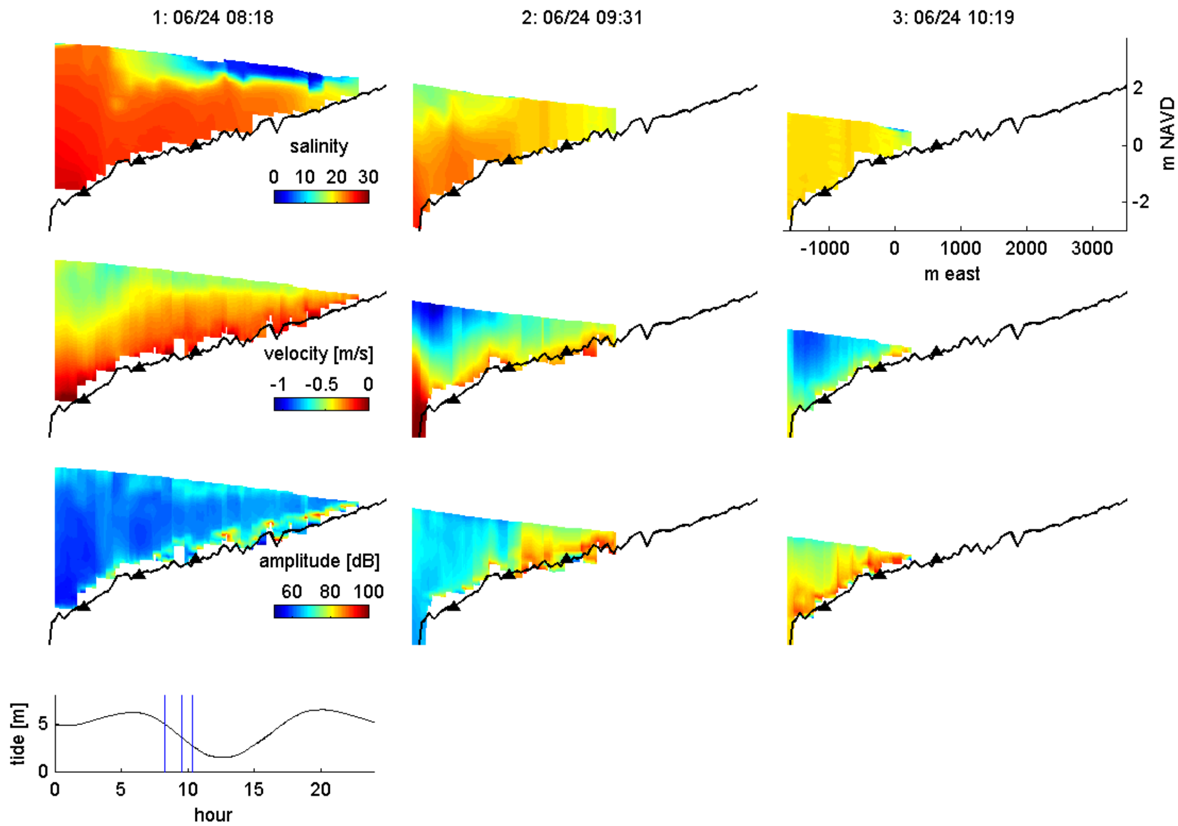

Figure 4. Three across-flats surveys of salinity (top), velocity (middle), and acoustic backscatter (bottom) during a spring ebb tide on June 24. Tidal elevation is shown in the lower left with the survey times indicated; positions of stations 1, 2, and 5 are marked with triangles on the transects. The sloping water surface reflects the change in water elevation during each transect.

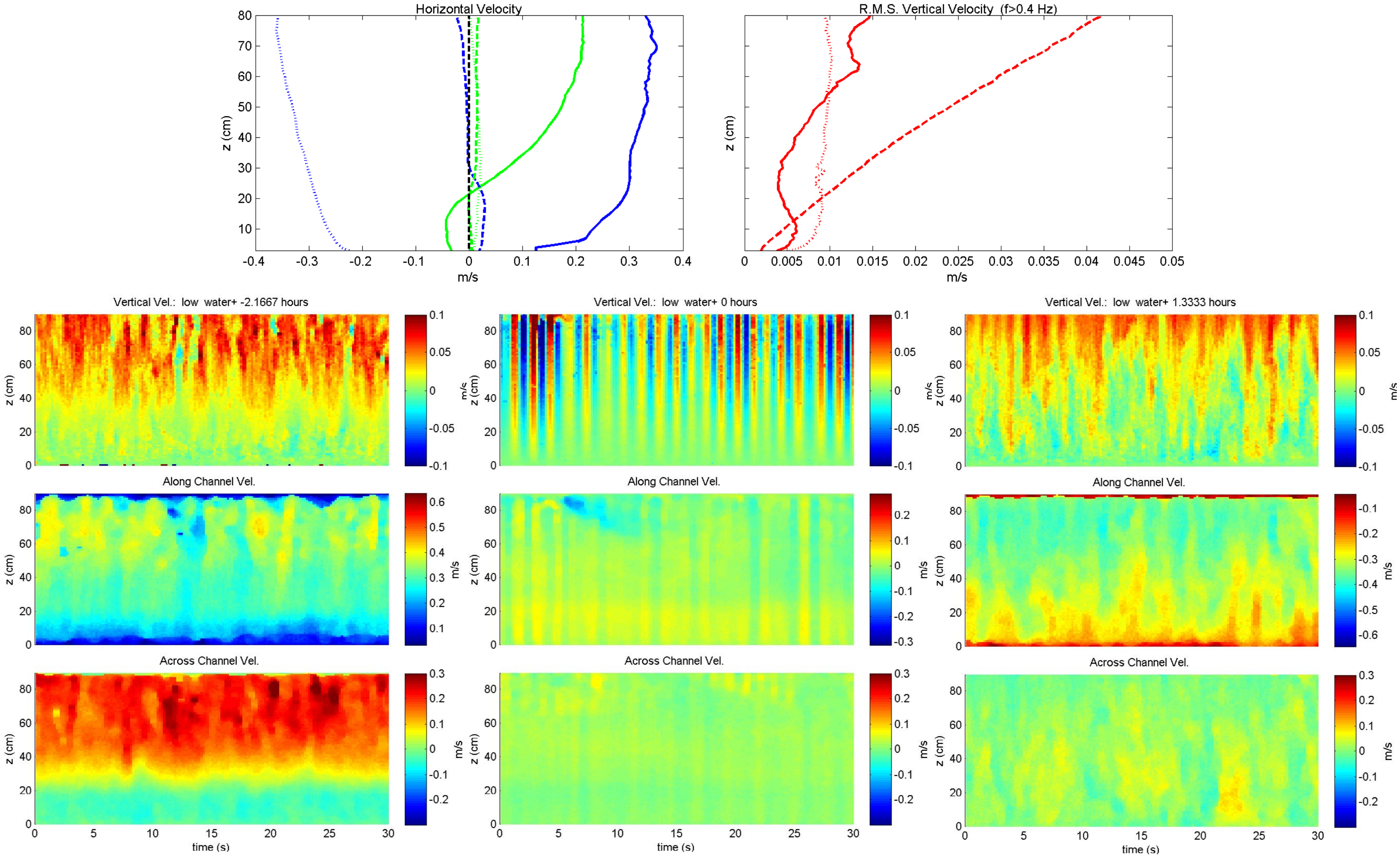

Figure 5. Examples of data from the PCADP. Upper panels: A. Profiles of horizontal velocity. Along channel velocities are blue lines, Across channel are green. Solid lines during Ebb tide, dashed lines are at slack low and dotted lines are during flood. The across-channel velocity (green) shows a jet of lateral velocity above 25 cmab, with a velocity reversal below 20 cmab, as water drains off the flats into the channel. B: R.M.S. vertical velocity for frequencies greater than 0.4 Hz with same line types as A. During Ebb water there is a minimum near the velocity reversal location of 25 cmab, and increased variations in the upper layer. During slack water short period waves (T= 1 s) dominate the vertical velocity and show the expected decay of velocity with depth. During flood, with decreased stratification, the vertical velocity variations are distributed more uniformly. Lower Panel: Color plots of vertical (top), along-channel (middle) and across-channel (lower), velocity vs. time and elevation above bottom for the same periods relative to slack low water as above. The left panels show the stratified turbulence and across channel velocity reversal during ebb; the middle panels show waves at slack low tide, and the right panels show more uniform, less stratified, turbulence.

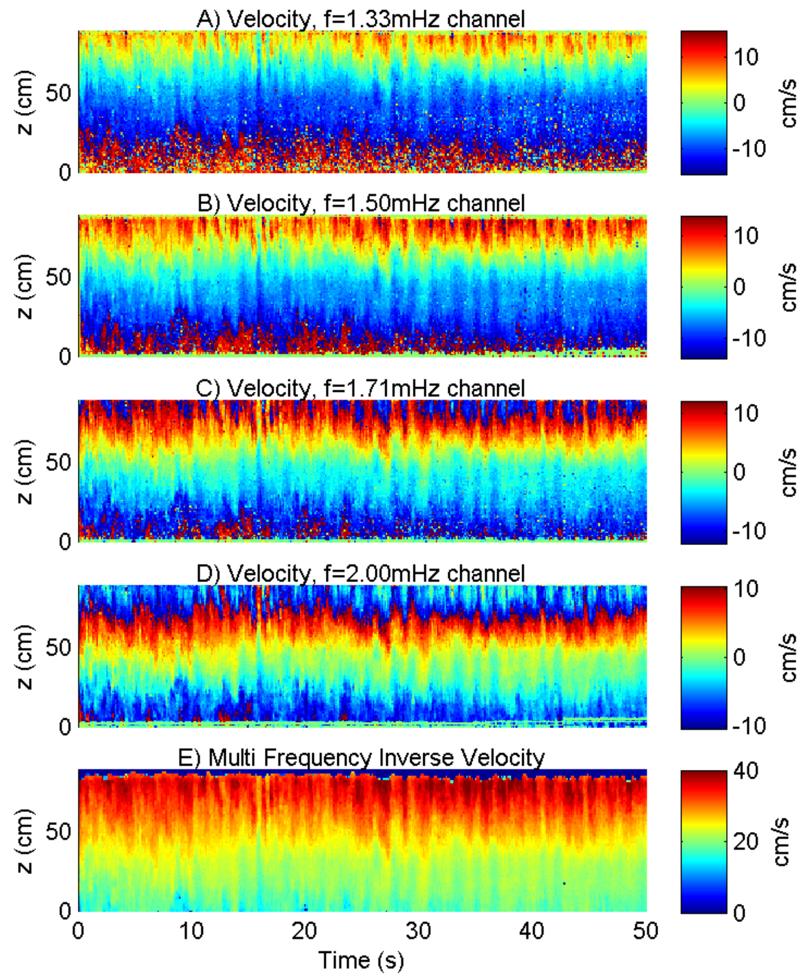

Figure 6. Multi-frequency pulse coherent Doppler data. Panels A through D show data from the individual frequencies (1.33, 1.50, 1.71, and 2.0 mHz) of the multi-frequency system. Velocity aliasing at 10 to 16 cm/s, depending on the frequency, can be clearly seen in all the individual channels. The aliasing seen near 80 cm above the bed in the 2.0 mHz data (E) is in fact a double wrap. The only non-aliased data in the individual frequencies is near the bed on the 1.33 (A) and 1.5 (B) mHz channels. The multi frequency inverse solution (E) is able to de-alias the data and produce high resolution data with along beam velocities of 10 to 40 cm/s (~ 1 m/s horizontal flow).

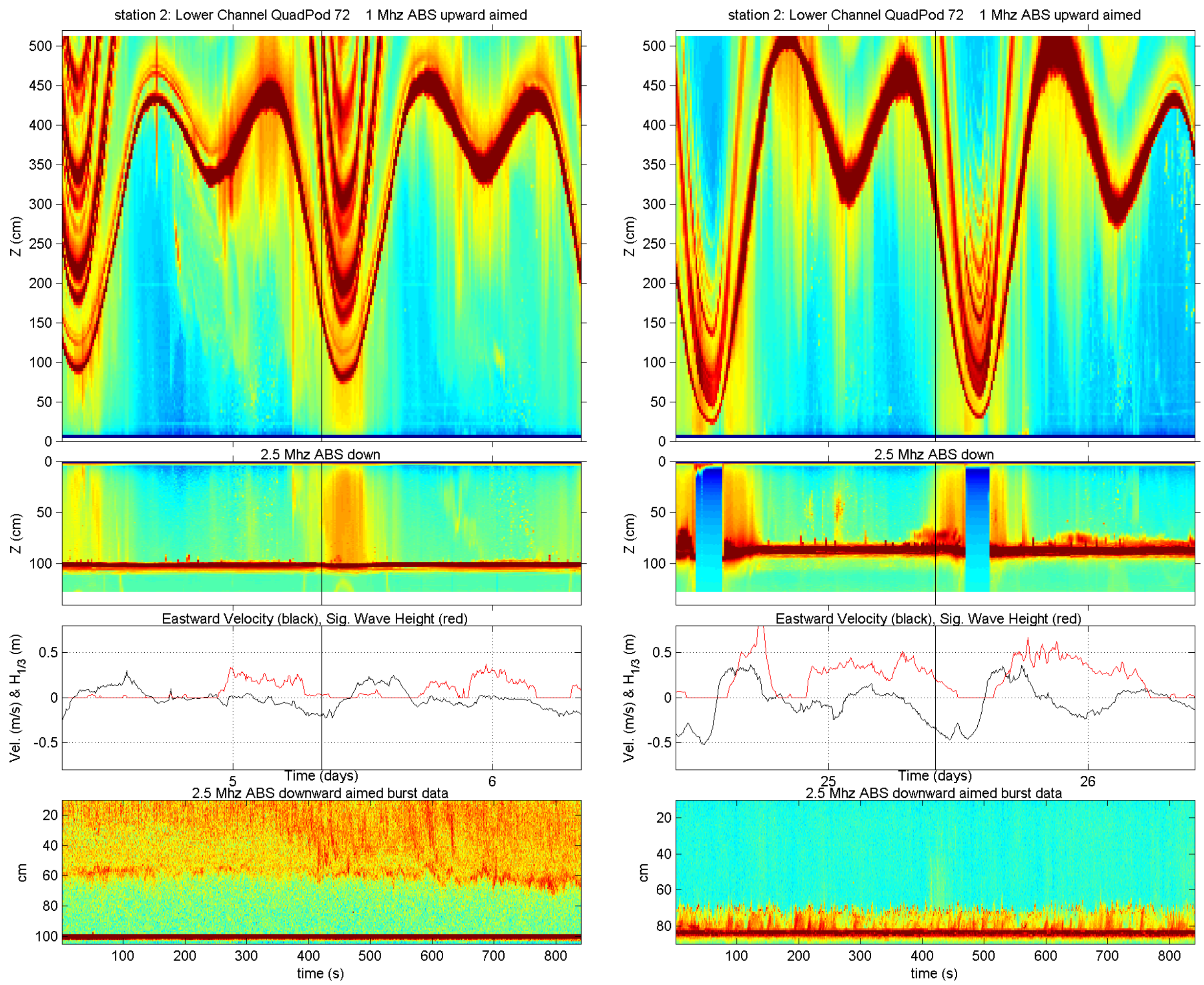

Figure 7. ABS data taken during ebb tide on March 5th (at the beginning of the deployment with high river discharge; left panels), and on March 5th (End of the deployment during lower river discharge, larger tides, and larger waves; right panels). The upper plots show two days of 1 mHz upward aimed burst averaged data showing acoustic reflections from the water surface and scattering from fine sediment and turbulent microstructure in the upper water column. The 2nd row of plots shows 2.5 mHz downward aimed burst averaged data, and the 3 rd row shows eastward velocity from an Nortek Vector ADV and significant wave height. The bottom row of plots show an individual burst (840 seconds of data) taken at the time indicated by the vertical black line in the other plots. In the left bottom panel, salinity stratification located 40 cmab prevents the high scattering water associated with the river plume from reaching the bed, and there is little sediment resuspended off the bed. In contrast, during more energetic conditions, shown on the right, near bed stratification contains the suspension in a near bed layer within 10 cm of the bed.